

## UC Davis

### UC Davis Previously Published Works

**Title**

Effects of Simulated Rare Earth Recycling Wastewaters on Biological Nitrification

**Permalink**

<https://escholarship.org/uc/item/3622b01p>

**Journal**

Environmental Science and Technology, 49(16)

**ISSN**

0013-936X

**Authors**

Fujita, Yoshiko  
Barnes, Joni  
Eslamimanesh, Ali  
et al.

**Publication Date**

2015-08-18

**DOI**

10.1021/acs.est.5b01753

Peer reviewed



# HHS Public Access

Author manuscript

*Environ Sci Technol.* Author manuscript; available in PMC 2017 April 04.

Published in final edited form as:

*Environ Sci Technol.* 2015 August 18; 49(16): 9460–9468. doi:10.1021/acs.est.5b01753.

## Effects of simulated rare earth recycling wastewaters on biological nitrification

Yoshiko Fujita<sup>1,\*</sup>, Joni Barnes<sup>1</sup>, Ali Eslamimanesh<sup>2</sup>, Malgorzata M. Lencka<sup>2</sup>, Andrzej Anderko<sup>2</sup>, Richard E. Riman<sup>3</sup>, and Alexandra Navrotsky<sup>4</sup>

<sup>1</sup>Idaho National Laboratory, Idaho Falls, ID 83415

<sup>2</sup>OLI Systems Inc., 240 Cedar Knolls Road, Suite 301, Cedar Knolls, NJ 07927

<sup>3</sup>Rutgers, The State University of New Jersey, Department of Materials Science and Engineering, 607 Taylor Road, Piscataway, NJ 08855

<sup>4</sup>Peter A. Rock Thermochemistry Laboratory and NEAT ORU, University of California Davis, Davis, CA 95616

### Abstract

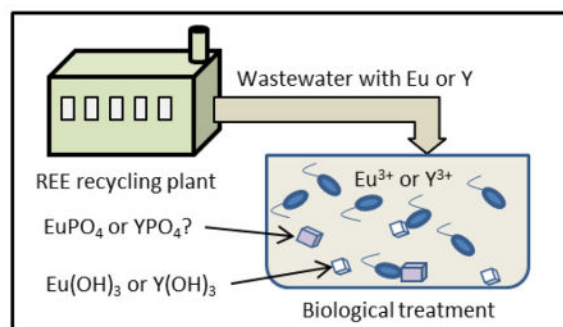
Increasing rare earth element (REE) supplies by recycling and expanded ore processing will result in generation of new wastewaters. In some cases disposal to a sewage treatment plant may be favored but plant performance must be maintained. To assess the potential effects of such wastewaters on biological treatment, model nitrifying organisms *Nitrosomonas europaea* and *Nitrobacter winogradskyi* were exposed to simulated wastewaters containing varying levels of yttrium or europium (10, 50 and 100 ppm), and the extractant tributyl phosphate (TBP, at 0.1 g/L). Y and Eu additions at 50 and 100 ppm inhibited *N. europaea*, even when virtually all of the REE was insoluble. Provision of TBP with Eu increased *N. europaea* inhibition, although TBP alone did not substantially alter activity. For *N. winogradskyi* cultures Eu or Y additions at all tested levels induced significant inhibition, and nitrification shut down completely with TBP addition. REE solubility was calculated using the previously developed MSE (Mixed-Solvent Electrolyte) thermodynamic model. The model calculations reveal a strong pH dependence of solubility, typically controlled by the precipitation of REE hydroxides but also likely affected by the formation of unknown phosphate phases, which determined aqueous concentrations experienced by the microorganisms.

### Graphical abstract

\*Corresponding Author Contact Information: yoshiko.fujita@inl.gov; Tel. (+1) 208-526-1242; Fax (+1) 208 526 0828, Yoshiko.fujita@inl.gov. Mail Stop: 83415-2203.

#### SUPPORTING INFORMATION

A detailed description of the MSE thermodynamic model and associated modeling parameters are presented in the Supporting Information, along with a figure showing the effects of the organic solvent. This material is available free of charge via the Internet at <http://pubs.acs.org>.

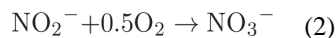
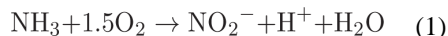


## Introduction

The increased global demand for rare earth elements (REE) and other elements critical for many renewable energy and other advanced technologies (e.g., magnets for wind turbines, electric vehicles, smart phones) has led to increased exploration for new sources and also interest in new methods for ore processing and refining, as well as for recycling of materials containing these strategic metals.<sup>1</sup> The expansion of REE production industries will be accompanied by growing volumes and new compositions of wastewater, for which companies will have to develop cost effective and sustainable disposal options. For some industrial generators, sending wastewater to a Publicly Owned Treatment Works (POTW), may be a desirable solution. However, wastewaters that jeopardize the performance of the POTW, in particular the biological modules, will not be acceptable. Biological wastewater treatment, mediated by highly efficient microbial communities adapted for this purpose, is a critical component in modern POTWs, enabling them to meet effluent discharge requirements.

Currently there are scant data regarding the impact of REE on biotic systems in general, and federal pretreatment standards for REE process wastewaters introduced into a POTW (40 CFR 421.275) do not include any REE-specific limits. Most of the reported studies examining interactions of REE and microbes have focused on biosorption of REE,<sup>2-7</sup> often as analogues for trivalent actinides.<sup>8,9</sup> However, some early studies have reported toxicity of REE to both bacteria and fungi.<sup>10</sup> In addition, high concentrations of cerium nitrate have been shown to inhibit the growth of Gram negative bacteria and fungi in treatment of burn wounds<sup>11</sup> and negative effects on soil microbes have been reported following application of REE containing fertilizers.<sup>12</sup> More recently, researchers have used *E. coli* to explore the antimicrobial mechanisms of REEs and reported toxicity at high concentrations of Ce, La and Pr.<sup>13-16</sup>

Biological wastewater treatment typically comprises both aerobic and anaerobic biological processes, and nitrification is a critical function of the aerobic module. It consists of the oxidation of ammonia to nitrite (reaction 1), and the subsequent oxidation of nitrite to nitrate (reaction 2) by a different set of bacteria.



Both ammonia and nitrite oxidizers are generally slow growing organisms that are sensitive to a variety of factors including temperature, pH, dissolved oxygen and chemical toxins such as heavy metals<sup>17–20</sup> and organic compounds including phenols, hydrocarbons and halogenated hydrocarbons.<sup>21, 22</sup> As a result, the nitrifying activity of activated sludge is more vulnerable to inhibition than other microbial conversions and, due to the slow growth rate of nitrifying bacteria, recovery of damaged sludge can be protracted and costly. Consequently pure cultures of nitrifying bacteria are frequently used to assess the inhibitory effects of industrial and pharmaceutical wastewaters on biological treatment systems.<sup>23–26</sup> Nitrification capacity is also an important measure of soil fertility; Xu and Wang (2001) studied the effect of an REE mixture (a commercial preparation for agricultural use) and La on ammonia oxidation in soil slurries.<sup>27</sup> They reported no observed effect concentrations of 393 and 432 mg kg<sup>-1</sup> for the mixture and La, respectively, and concluded that REE fertilizer additions did not significantly impact soil health. However, REE speciation and concentrations were not examined.

In this report, we present results from pure culture studies using two nitrifying bacterial species, *Nitrosomonas europaea* and *Nitrobacter winogradskyi*, exposed to REE. *N. europaea* is an ammonia oxidizer, and *N. winogradskyi* is a nitrite oxidizer. The bacterial cultures were challenged with synthetic wastewaters containing yttrium or europium. Residuals of these REE would be expected to remain in wastewater generated during recycling of fluorescent light phosphor powders. Phosphor recycling has significant potential for near-term commercial recovery of REEs, due to the high content of Y, Eu and Tb in fluorescent lamp phosphors, the large volume of lamps already in use, and the existing end-of-life recycling infrastructure.<sup>1</sup> Hence, if phosphor recycling is implemented at industrial scale, POTWs may well receive increasing loads of wastewaters from phosphor REE recyclers.

The bacterial cultures were exposed to varying levels of either Y or Eu and effects on nitrification activity were measured over time. In addition, experiments were conducted in the presence or absence of tributyl phosphate (TBP), a common solvent used for the extraction of REE from aqueous solutions. Because of TBP's high viscosity (3.399 mPa.s at 25°C,<sup>28</sup> compared to 0.890 mPa.s for water<sup>29</sup>), it is typically used in a mixture with an alkane; for our experiments we utilized a mixture of TBP and the isoparaffin solvent Isopar™ L.

In order to understand the effects of experimental conditions (e.g., pH, total REE concentration and the presence of TBP) on the nitrification processes, it is important to predict the aqueous solubility of the REE as a function of those experimental conditions. Such predictions can be obtained from a thermodynamic model that is accurately

parameterized to reflect solution speciation including acid-base equilibria, complexation and precipitation of solid phases. Although various kinetically-controlled phenomena (e.g., slow precipitation of solid phases or adsorption) can influence the availability of REEs, equilibrium solubility provides a foundation for understanding the behavior of REEs. A suitable framework for our experimental system was provided by the previously developed Mixed-Solvent Electrolyte (MSE) model.<sup>30, 31</sup> This model combines an equation of state for standard-state properties of individual species, an excess Gibbs energy model, and an algorithm for solving phase and chemical equilibria in multiphase systems. Although there is a scarcity of well-documented thermodynamic solubility data in the open literature for Eu and Y in acidic and TBP-containing solutions, the MSE framework<sup>30, 31</sup> enabled us to leverage available data and generate reasonable predictions.

## Materials and Methods

### Chemicals

Unless specified otherwise, all chemicals used were ACS reagent grade. Yttrium oxide (99.99%) was purchased from Research Chemicals (Phoenix, AZ) and europium chloride (99.99%) from Strem Chemicals, Inc. (Newburyport, MA). Tributyl phosphate was provided within a commercial isoparaffin matrix (Isopar™ L, from ExxonMobil), as a 30:70 (v/v) mixture.

### Bacterial cultures

*Nitrosomonas europaea* (ATCC 19718) and *Nitrobacter winogradskyi* (ATCC 25391) cultures were obtained from the American Type Culture Collection. The *N. europaea* strain was routinely cultivated in a defined mineral medium described by Sato et al.<sup>32</sup> The *N. winogradskyi* strain was routinely cultivated in medium (SW) described by Soriano and Walker.<sup>33</sup> Both cultures were grown at 30°C in the dark with rotary shaking (100 rpm).

### Synthetic wastewater composition

The synthetic wastewater consisted of Y<sub>2</sub>O<sub>3</sub> or EuCl<sub>3</sub> dissolved in 0.1 M HCl, in amounts that would result in 0, 10, 50, or 100 ppm of the respective metal in the exposure experiments. In some of the experiments, TBP in Isopar™ L was included at final concentration of 100 ppm as TBP (approximate solubility of TBP in water at 25°C is 400 ppm).<sup>34</sup> No liquid phase separation was observed in the experiments.

### REE and TBP exposure experiments

The experiments were conducted in 250 ml baffled Erlenmeyer flasks with closures allowing air exchange. To each flask, 15 ml of the synthetic wastewater were added. Then, because in an activated sludge system with nitrification the optimum pH is generally between 7 and 8,<sup>35</sup> the pH was adjusted to pH 7.5–8.0 with NaOH. Next, 60 ml of either Sato medium (for *N. europaea*) or SW medium (for *N. winogradskyi*) were added to each flask. For the biotic experiments, the medium was pre-inoculated (5% v/v) with 48 h cultures of the bacteria (initial cell densities in flasks estimated at  $\sim 8.0 \times 10^5$  cells/mL for *N. europaea*;  $\sim 6.0 \times 10^5$  cells/mL for *N. winogradskyi*). The effects of TBP (100 ppm) were also tested on each culture, along with the Isopar™ L alone. For the *N. europaea*, TBP was also tested together

with Eu. For the *N. winogradskyi*, TBP was provided together with Y. Biotic treatment flasks were set up in triplicate, with one abiotic (no cell) control for each experimental condition. The flasks were incubated at 30°C in the dark, with shaking (100 rpm). At 0, 24, 48 and 72 h, samples (2 ml) were taken for pH and nitrite measurements. At 72 hours, samples (10 ml) were collected and filtered (0.22 micron) for REE measurement.

### Analytical methods

Nitrite was measured using American Public Health Association Standard Method 4500-NO<sub>2</sub>-B.<sup>36</sup> REE concentrations were measured using inductively coupled plasma mass spectrometry (ICP-MS). The instrument (iCAP Q, Thermo Scientific) was standardized and operated in accordance with manufacturer instructions. Ultrapure concentrated nitric acid was used to acidify (1%) the filtered samples as well as the commercial standard stock solutions prior to ICP-MS analysis.

### Thermodynamic speciation calculations

The solubilities of Y and Eu in the synthetic aqueous solutions were predicted using the MSE thermodynamic model.<sup>30, 31</sup> This model is described in the Supporting Information. The parameters of the MSE model<sup>30, 31</sup> were determined by analyzing and regressing available thermodynamic data. Table 1 shows the sources of the experimental data, data types, temperature, pressure and ranges of REE distribution coefficient data.

An important constraint in the data regression was the fact that available data for the Y/Eu + TBP + acid + H<sub>2</sub>O solutions were limited to a few sets of distribution coefficients for the REE between the aqueous phase and the organic (TBP-rich) phase. Therefore, first it was necessary to determine the model parameters representing the liquid-liquid equilibrium (LLE) data for the TBP + acid + H<sub>2</sub>O systems. For this purpose, experimental LLE data for the TBP + HNO<sub>3</sub>/HCl/HClO<sub>4</sub> aqueous solutions were regressed to obtain the interaction parameters.

The second step was to represent the solubility data for various inorganic REE species including hydroxides, chlorides, and phosphates. Since the REE hydroxides are likely to precipitate rapidly (compared to measurement time) in the experimental media, the accuracy of parameters for Y(OH)<sub>3</sub> and Eu(OH)<sub>3</sub> is particularly important. To the best of our knowledge, the only relevant data in the open literature for Y(OH)<sub>3</sub> are the solubility products (K<sub>sp</sub>) for the freshly precipitated and aged hydroxides in various aqueous solutions. To obtain reproducible and predictive thermodynamic parameters, K<sub>sp</sub> values for aged Y(OH)<sub>3</sub> and aqueous solubility data for aged Eu(OH)<sub>3</sub> were chosen and regressed.

It is well established in the literature that TBP forms neutral complexes with REE with the general formula REEA<sub>m</sub>TBP<sub>n</sub> where A is an anion, and values for m and n depend on the chemical solvation mechanism for REE extraction in a specific system.<sup>37–39</sup> Such complexes play a key role in extraction-based separation processes. One of the dominant anions in the media studied here that also could potentially take part in a complex with TBP is chloride. However, only one data point was found in the literature pertaining to the distribution of Eu between an HCl-containing aqueous phase and a TBP organic phase<sup>40</sup> whereas data sets for the Y/Eu + HNO<sub>3</sub>/HClO<sub>4</sub> aqueous solutions with TBP are more abundant. Therefore, data

for various systems were combined to obtain the best estimates of complexation parameters. The methodology adopted to determine the required model parameters is described in the Supporting Information. The thermodynamic model parameters that were derived and or used in this study are also presented therein, in Tables S1–S4.

## Results and Discussion

### Effects of REEs on ammonia oxidation by *N. europaea*

*N. europaea* activity was monitored by measuring nitrite production over time; other researchers have reported that nitrite production correlates well with growth for *N. europaea*,<sup>32, 41</sup> and this was confirmed in preliminary experiments conducted in our laboratory (data not shown). Nitrite production was not detected in any of the abiotic controls, and therefore such data are not shown in the figures or discussed further.

Nitrite production during the experiments exposing *N. europaea* to 10, 50, and 100 ppm Eu is shown in Figure 1a. The results indicated that Eu at 10 ppm had little or no impact on *N. europaea* metabolism, but higher Eu loadings were inhibitory; by 72 h the average ammonia oxidation activities relative to the no Eu control were  $83.8 \pm 3.0\%$  and  $79.8 \pm 4.0\%$ , respectively, for 50 and 100 ppm Eu. Effects on metabolism were also reflected in the measured pH values for the cultures. Ammonia oxidation by molecular oxygen is an acid producing reaction, as shown in equation 1, and in the cultures with active ammonia oxidation the pH dropped from the initial values ( $> 7.5$ ) to 6.0–6.5 by 48 h. By 72 h the average pH of the 0 and 10 ppm Eu cultures was 6.1. At this pH, nitrification is expected to be suboptimal, but can still occur.<sup>23</sup> Acidification also occurred in the 50 and 100 ppm cultures but more slowly. By 72 h, the 50 and 100 ppm Eu cultures had an average pH of  $\sim 6.5$ .

The effect of yttrium at 10 ppm was similar to that of Eu (i.e., negligible impact), but at 50 and 100 ppm the inhibitory effect of Y was comparatively much greater than Eu (Figure 1b). With the addition of 50 and 100 ppm Y, final nitrite production values were  $34.1 \pm 4.1\%$  and  $21.4 \pm 0.8\%$ , respectively, compared to the no Y control. The different observed effects for the two REE may reflect the greater molar amounts of Y exposed to the organisms compared to Eu; the lower atomic mass of Y results in equivalent masses of the elements corresponding to 70% greater Y than Eu in terms of moles. Again, the inhibition was manifested in the pH of the cultures; initial pH values of  $\sim 7.5$  dropped to  $\sim 6.1$  by 72 h in the 0 and 10 ppm Y cultures, but the pH remained unchanged in the 50 and 100 ppm cultures.

### Effects of REEs on nitrite oxidation by *N. winogradskyi*

Activity of the *N. winogradskyi* cultures was monitored by measuring nitrite disappearance over time. Analogous to the case for *N. europaea*, no nitrifying activity was detected in the abiotic controls, and therefore those data are not discussed further.

Compared to *N. europaea*, *N. winogradskyi* appeared to be more sensitive to Eu (Figure 1c). Nitrite consumption was inhibited even at 10 ppm Eu; by 72 hours, the relative nitrite consumption compared to the no Eu control was  $34.5 \pm 2.2\%$ . The corresponding values for the 50 and 100 ppm Eu cultures were  $29.3 \pm 8.1\%$  and  $17.2 \pm 1.4\%$ , respectively.

Yttrium also had a deleterious effect (Figure 1d), and 10 ppm Y inhibited the cultures to a similar extent as the 10 ppm Eu; the relative nitrite consumption compared to the no Y control was  $36.2 \pm 4.9\%$ . As was observed for the *N. europaea*, the *N. winogradskyi* treatments receiving the 50 and 100 ppm amendments of Y were more inhibited than the corresponding treatments receiving Eu; relative nitrite consumption values were  $4.3 \pm 0.9\%$  and  $2.8 \pm 1.2\%$  for 50 ppm Y and 100 ppm Y, respectively.

### Effects of TBP on nitrification activity

When provided to *N. europaea*, TBP and Isopar™ L alone appeared to slightly inhibit nitrite production initially, but by 72 h the cultures seemed to have almost completely “recovered” (Figure S2 in Supporting Information). However, when TBP was added together with Eu, there appeared to be a synergistic effect--the inhibition by the metal was even greater (Figure 2a). In these cultures, nitrification inhibition was also exhibited in the pH; at 72 h the average pH of the 10 ppm Eu + TBP cultures was ~6.5, and in the 50 and 100 ppm Eu cultures with TBP the final pH values remained at or above pH 7.5.

In contrast to *N. europaea*, *N. winogradskyi* appeared to be extremely sensitive to TBP. In fact no nitrite consumption was observed in any of the cultures provided with 0.1 g/L TBP (Figure 2b). The effect appeared to be specific to TBP; when Isopar™ L alone was provided to *N. winogradskyi*, the cultures showed no inhibition compared to the controls with no added Y or organics (Figure S2).

The mechanism(s) of toxicity for TBP on *N. europaea* and *N. winogradskyi* are unknown. For the *N. europaea*, where the TBP enhanced inhibition by REE, the effect may have been related to increased aqueous solubility of the REE, as predicted by the model simulations (discussed below). In addition, perhaps TBP facilitated transfer of the metals into or through the cell membrane, consistent with TBP's role in solvent extraction of REE and actinides from aqueous solutions. With respect to the observed toxicity of TBP to *N. winogradskyi*, although researchers have shown that TBP can be tolerated and degraded by both pure and mixed microbial cultures, <sup>42–46</sup> concentrations above 0.1 g/L were reportedly toxic to *Pseudomonas putida*.<sup>47</sup> Kulkarni et al. found that TBP induced oxidative stress and DNA damage in a *Klebsiella* strain, although the organism could also grow on 1 g/L TBP if other nutrients were provided.<sup>48</sup>

### Prediction and measurement of REE solubility in aqueous solution

As mentioned earlier, REE hydroxide precipitation plays a key role in determining soluble REE levels. While the actual REE concentration in a given system may be lower than the solubility of REE hydroxides due to the precipitation of other phases or adsorption phenomena, it is not likely to exceed it. Thus, REE hydroxide solubility provides a useful upper bound for the available REE concentration. Prior to applying the model to the experimental systems, we verified the accuracy of model predictions for the solubility of Eu and Y hydroxides. Verification details are in the Supporting Information.

Upon confirmation that the model was acceptable for predicting Eu and Y solubility in simple aqueous solutions, we applied it to interpretation of the experimental data. In the *N. europaea* experiments (Sato medium), pH changes were expected to result in significant



changes to aqueous Eu and Y concentrations. At the initial pH conditions (pH 7.5–8.0), with either Eu or Y, >98% of the REE added to any of the experimental treatments was expected to be insoluble (see Figures 3 and 4, solid lines). At pH 7.5, the expected soluble Eu concentration was approximately 67 ppb for all 3 treatment levels (solid line, Figure 3). However, under the final pH conditions for the Eu-amended cultures (pH ranging from 6.1 to 6.5), significantly more of the Eu was expected to be soluble. Some soluble Eu was measured in the 50 and 100 ppm treatments with pH < 7, but only 1–3 ppb, less than 1% of expected. In the corresponding 50 and 100 ppm treatments with TBP where the pH remained higher (>7.3), Eu remained below detection (1 ppb) despite the higher predicted solubility due to TBP (dashed lines in Figure 3). Figure 3 shows two Eu data clusters in the Sato medium. One cluster in the pH range of 8.5–9.0 is consistent with the solubility of  $\text{Eu}(\text{OH})_3$ , whereas the second cluster at lower pH values could be attributable to precipitation of a different mineral with lower solubility, namely a phosphate phase ( $\text{EuPO}_4$ ). The Sato medium contains 5 mM phosphate. The solubility of the phosphate phase (dash-dotted lines in Figure 3) is predicted to be substantially lower than that of the  $\text{Eu}(\text{OH})_3$ . The fact that the second data cluster lies between the  $\text{Eu}(\text{OH})_3$  and  $\text{EuPO}_4$  solubility curves suggests that the observed concentrations reflect slow, incomplete formation of a phosphate phase. The freshly precipitated mineral may or may not have the same stoichiometry as the stable  $\text{EuPO}_4$  phase. Identification of such a phase would require further experimental studies.

For the yttrium experiments with *N. europaea*, at pH 7.5 the soluble Y concentration was expected to be 147 ppb in all three Y-amended treatments. Based on the measured pH, significant soluble Y concentrations after 72 hours were expected in the 10 ppm Y cultures. However, a quantifiable level (>0.5 ppb) of soluble Y was observed in only one of the three replicates; the measured value was 9.7 ppb for a sample at pH 6.1. At that pH, all of the added Y was expected to be soluble (see solid curve in Figure 4). Again, it appears likely that slow precipitation of a phosphate mineral is the cause of the low aqueous Y concentrations.

In the *N. winogradskyi* experiments (SW medium), nitrite oxidation was not expected to alter the pH (equation 2). At 72 hours the pH of the cultures with Eu remained relatively unchanged from the initial pH range 7.5–8.0. Aqueous Eu concentrations were expected to be 45 ppb under all three Eu amendment conditions (Figure 5). For the 100 ppm Eu treatments, biotic and abiotic, the measured aqueous Eu values ranged between 21 and 43 ppb, and for the treatments with 10 and 50 ppm Eu additions, the measured Eu was <10 ppb. These values were slightly lower than expected from  $\text{Eu}(\text{OH})_3$  solubility, suggesting that in this system too a phosphate mineral phase occurs. However, the SW medium contains much less phosphate (0.6 mM) than the Sato medium (5 mM). This is reflected in the smaller discrepancy between measured Eu and Eu predicted based solely on  $\text{Eu}(\text{OH})_3$  solubility (solid lines in Figure 5); in other words  $\text{EuPO}_4$  precipitation plays a smaller role than in the Sato medium, for given REE amounts. The formation of the different phases is controlled by the amount of the phosphate available relative to the REE. If the total available REE exceeds the phosphate, the phosphate will be predicted to precipitate almost completely and the remaining REE may form a hydroxide phase. Then, the aqueous REE concentration will be controlled by the REE hydroxide solubility. This is evident in Figure 5 for the case where the total Eu is 100 ppm (0.66 mM), exceeding the total phosphate (0.6 mM) in the medium.

The impact of phosphate mineral formation was also observed in the *N. winogradskyi* experiments with Y. Here too measured Y concentrations appeared to be controlled largely by  $Y(OH)_3$  solubility (Figure 6, solid lines). The predicted increased REE solubility in the presence of TBP (dashed lines) was supported by the limited data available; for example, in 50 ppm Y treatments at pH 7.7, the measured aqueous Y concentrations in the presence and absence of TBP were 156 and 83 ppb, respectively. Nevertheless, phosphate mineral precipitation had a greater impact on Y solubility than TBP. In Figure 6, the effect of phosphate precipitation was most obvious (larger deviation downward from the solid line) in the samples with the least added Y (10 ppm). Additional putative evidence for the kinetically delayed precipitation of a Y phosphate phase was an observed drop in pH to 7.3 for some of the 50 and 100 ppm treatments over the first 24 hours. A pH drop would not be as evident for the 10 ppm Y case, where a smaller amount of Y phosphate could precipitate.

The role of phosphate is important in considering the inhibition results for the two cultures: in the lower phosphate SW medium, the *N. winogradskyi* were exposed to higher soluble Eu and Y concentrations. This was particularly evident in the 100 ppm REE experiments, where the predicted initial (pH 7.5) aqueous concentrations were  $4.7E-10$  ppb in Sato and 44 ppb in Soriano for Eu, and  $8.8E-2$  ppb in Sato and 92 ppb in Soriano medium for Y. In the 10 and 50 ppm experiments, the difference between the predicted soluble concentrations was much smaller, and absolute concentrations were also far smaller: Eu concentrations ranged between a low of  $4.4E-10$  ppb in the 10 ppm Sato medium and  $9.3E-9$  ppb in the 50 ppm SW medium. Similarly, Y concentrations ranged between  $8.0E-10$  ppb and  $5E-7$  ppb.

In addition to the precipitation of phosphate minerals, another possible reason for the lower than expected (based on hydroxide mineral solubility) aqueous concentrations of both Eu and Y is that the REE were adsorbed onto bacterial cell surfaces. Sorption of REE on bacterial cells, even at low pH (i.e.,  $pH < 3$ ), is well known.<sup>49–52</sup> However, when cell-free samples of the Sato medium amended with 10 ppm Eu were acidified to pH 6, Eu remained non-detectable in solution ( $< 0.1$  ppb), indicating that it was not available for biosorption under these conditions.

## Implications

Our experimental results indicate that Eu and Y at  $>10$  ppm can inhibit ammonia oxidizing activity by *N. europaea*, even when most of the REE are removed from solution by precipitation. The nitrite oxidizer *N. winogradskyi* is more sensitive; 10 ppm Eu or Y caused more than 50% inhibition compared to the no REE controls. How the REE exert toxicity on these nitrifiers is unknown. Hu et al. reported that for Ni, Zn and Cd, nitrifier inhibition was correlated with intracellular concentrations, while  $Cu^{2+}$  appeared to exert toxicity by disrupting cell membranes.<sup>53</sup> Genes associated with oxidative stress were observed to be upregulated in *N. europaea* exposed to Zn and Cd.<sup>20</sup> Peng and coworkers reported that for *E. coli*,  $La^{3+}$  (400 ppm) disrupted the outer membrane, perhaps by displacing  $Ca^{2+}$  and  $Mg^{2+}$  ions from surface lipopolysaccharides.<sup>16</sup> The same research group also reported that  $Pr^{3+}$  (at 1 mM) increased *E. coli* permeability to  $Cu^{2+}$  ions.<sup>15</sup> Increased membrane permeability was also cited by others as a cause for *E. coli* mortality when exposed to cerium nitrate at concentrations  $> 0.25$  mM (equivalent to 35 ppm Ce).<sup>13, 14</sup>

One of our most interesting observations was that the addition of greater amounts of Eu or Y led to greater inhibition, even when the changes in the REE aqueous concentrations were predicted to be negligible. This suggests that the organisms are exquisitely sensitive to REE (sensing, for example, an increase from 4.4E-10 to 4.5E-10 ppb Eu, in going from the 10 ppm to 50 ppm treatments in the Sato medium), or insoluble species may contribute toxicity. The mechanism(s) by which insoluble Eu or Y could exert a toxic effect on the bacterial species is(are) unknown; an intriguing possibility is the formation of intracellular Eu or Y nanoparticles that could promote detrimental reactions on their surfaces.<sup>54</sup> Effects could also be exerted extracellularly; Yuan et al. recently posited that adsorbed lead contributed to inhibition of activated sludge microorganisms, and that total Pb was a better predictor of toxicity than soluble Pb.<sup>55</sup>

Our findings also indicated that REE themselves may not be the only components of concern in a REE beneficiation or recycling wastewater with respect to biological wastewater treatment. Organic compounds used for selective extraction of REE from aqueous process streams may also jeopardize biological treatment performance. The organic complexant TBP at 0.1 g/L, which is below its solubility limit in water (at which concentration it would be expected to be present in a wastewater from a solvent extraction process) appeared to increase inhibition of *N. europaea* by Eu, possibly by enhancing transport of the REE into the cells. On the other hand, with *N. winogradskyi*, no nitrifying activity at all was detected in the presence of TBP, whether the REE tested (Y) was present or not.

Future research by our group will also include the examination of the impacts of Eu and Y and organic complexants (TBP and or other ligands) on microbial consortia from an operating wastewater treatment plant. It is possible that such consortia will be more resilient than the single species tested here, with respect to toxic effects of REE beneficiation or recycling wastewaters. Research in this area contributes to broader understanding of the behavior of REE in ecosystems outside of wastewater treatment plants. With the rapid proliferation of REE -dependent products in the electronics and clean energy fields, unintended direct releases of REE to the environment from industrial or mining operations as well as releases following disposal of REE-containing consumer products (e.g., landfill leachates) are almost certain to increase. Improved understanding of their behavior in the environment and effects on biotic systems are necessary to assess risk and to support the development of remediation methods if necessary.

## Supplementary Material

Refer to Web version on PubMed Central for supplementary material.

## Acknowledgments

We express our appreciation to D. LaCroix and J. Taylor at the University of Idaho/Center for Advanced Energy Studies for ICP-MS measurements. We also thank M. Greenhalgh of INL for advice regarding wastewater composition and for provision of the TBP and Isopar<sup>TM</sup> L. We also thank anonymous reviewers for their helpful comments. This research is supported by the Critical Materials Institute, an Energy Innovation Hub funded by the U.S. Department of Energy, Office of Energy Efficiency and Renewable Energy, Advanced Manufacturing Office. Funding was provided via the DOE Idaho Operations Office Contract DE-AC07-05ID14517.

## References

1. Binnemans K, Jones PT, Blanpain B, Van Gerven T, Yang YX, Walton A, Buchert M. Recycling of rare earths: a critical review. *J Clean Prod.* 2013; 51:1–22.
2. EPA, U. S. Rare Earth Elements: A review of production, processing, recycling, and associated environmental issues. 2012.
3. Merten D, Kothe E, Buechel G. Studies on microbial heavy metal retention from uranium mine drainage water with special emphasis on rare earth elements. *Mine water and the environment.* 2004; 23:34–43.
4. Ngwenya BT, Magennis M, Olive V, Mosselmans JFW, Ellam RM. Discrete Site Surface Complexation Constants for Lanthanide Adsorption to Bacteria As Determined by Experiments and Linear Free Energy Relationships. *Environ Sci Technol.* 2010; 44(2):650–656. [PubMed: 20000843]
5. Ngwenya BT, Mosselmans JFW, Magennis M, Atkinson KD, Tournay J, Olive V, Ellam RM. Macroscopic and spectroscopic analysis of lanthanide adsorption to bacterial cells. *Geochim Cosmochim Acta.* 2009; 73(11):3134–3147.
6. Texier AC, Andres Y, Faur-Brasquet C, Le Cloirec P. Fixed-bed study for lanthanide (La, Eu, Yb) ions removal from aqueous solutions by immobilized *Pseudomonas aeruginosa*: experimental data and modelization. *Chemosphere.* 2002; 47(3):333–342. [PubMed: 11996155]
7. Texier AC, Andres Y, Le Cloirec P. Selective biosorption of lanthanide (La, Eu, Yb) ions by *Pseudomonas aeruginosa*. *Environ Sci Technol.* 1999; 33(3):489–495.
8. Markai S, Andres Y, Montavon G, Grambow B. Study of the interaction between europium (III) and *Bacillus subtilis*: fixation sites, biosorption modeling and reversibility. *J Colloid Interface Sci.* 2003; 262(2):351–361. [PubMed: 16256615]
9. Ozaki T, Suzuki Y, Nankawa T, Yoshida T, Ohnuki T, Kimura T, Francis AJ. Interactions of rare earth elements with bacteria and organic ligands. *J Alloys Compounds.* 2006; 408:1334–1338.
10. Talbert D, Johnson G. Some effects of rare earth elements and yttrium on microbial growth. *Mycologia.* 1967; 59:492–503.
11. Monafó WW, Tandon SN, Ayvazian VH, Tuchschild J, Skinner AM, Deitz F. Cerium nitrate: a new topical antiseptic for extensive burns. *Surgery.* 1976; 80(4):465–73. [PubMed: 135364]
12. Hu X, Ding Z, Chen Y, Wang X, Dai L. Bioaccumulation of lanthanum and cerium and their effects on the growth of wheat (*Triticum aestivum L.*) seedlings. *Chemosphere.* 2002; 48(6):621–629. [PubMed: 12143937]
13. Chen A, Shi Q, Feng J, Ouyang Y, Chen Y, Tan S. Dissociation of outer membrane for *Escherichia coli* cell caused by cerium nitrate. *J Rare Earths.* 2010; 28(2):312–315.
14. Chen A, Shi Q, Ouyang Y, Chen Y. Effect of Ce<sup>3+</sup> on membrane permeability of *Escherichia coli* cell. *J Rare Earths.* 2012; 30(9):947–951.
15. Peng L, Weiying Z, Xi L, Yi L. Structural basis for the biological effects of Pr (III) ions: alteration of cell membrane permeability. *Biol Trace Elem Res.* 2007; 120(1–3):141–147. [PubMed: 17916966]
16. Peng L, Yi L, Zhexue L, Juncheng Z, Jiabin D, Daiwen P, Ping S, Songsheng Q. Study on biological effect of La<sup>3+</sup> on *Escherichia coli* by atomic force microscopy. *J Inorg Biochem.* 2004; 98(1):68–72. [PubMed: 14659634]
17. Chandran K, Love NG. Physiological State, Growth Mode, and Oxidative Stress Play a Role in Cd(II)-Mediated Inhibition of *Nitrosomonas europaea* 19718. *Appl Environ Microbiol.* 2008; 74(8):2447–2453. [PubMed: 18245236]
18. Lee Y-W, Ong S-K, Sato C. Effects of heavy metals on nitrifying bacteria. *Water Sci Technol.* 1997; 36(12):69–74.
19. Sato C, Schnoor JL, McDonald DB. Characterization of effects of copper, cadmium and nickel on the growth of *Nitrosomonas europaea*. *Environ Toxicol Chem.* 1986; 5(4):403–416.
20. Park S, Ely RL. Candidate Stress Genes of *Nitrosomonas europaea* for Monitoring Inhibition of Nitrification by Heavy Metals. *Appl Environ Microbiol.* 2008; 74(17):5475–5482. [PubMed: 18606795]

21. Keener WK, Arp DJ. Kinetic Studies of Ammonia Monooxygenase Inhibition in *Nitrosomonas europaea* by Hydrocarbons and Halogenated Hydrocarbons in an Optimized Whole-Cell Assay. *Appl Environ Microbiol.* 1993; 59(8):2501–2510. [PubMed: 16349014]
22. Kim KT, Kim IS, Hwang SH, Kim SD. Estimating the combined effects of copper and phenol to nitrifying bacteria in wastewater treatment plants. *Water Res.* 2006; 40(3):561–568. [PubMed: 16442584]
23. Grunditz C, Dalhammar G. Development of nitrification inhibition assays using pure cultures of *Nitrosomonas* and *Nitrobacter*. *Water Res.* 2001; 35(2):433–440. [PubMed: 11228996]
24. Grunditz C, Gumaelius L, Dalhammar G. Comparison of inhibition assays using nitrogen removing bacteria: application to industrial wastewater. *Water Res.* 1998; 32(10):2995–3000.
25. Wang S, Gunsch CK. Effects of selected pharmaceutically active compounds on the ammonia oxidizing bacterium *Nitrosomonas europaea*. *Chemosphere.* 2011; 82(4):565–572. [PubMed: 20980043]
26. Williamson KJ, Johnson DG. A bacterial bioassay for assessment of wastewater toxicity. *Water Res.* 1981; 15(3):383–390.
27. Xu X, Wang Z. Effects of lanthanum and mixtures of rare earths on ammonium oxidation and mineralization of nitrogen in soil. *Eur J Soil Sci.* 2001; 52(2):323–329.
28. Tian Q, Liu H. Densities and Viscosities of Binary Mixtures of Tributyl Phosphate with Hexane and Dodecane from (298.15 to 328.15) K. *J Chem Engin Data.* 2007; 52(3):892–897.
29. Kestin J, Khalifa HE, Correia RJ. Tables of the dynamic and kinematic viscosity of aqueous NaCl solutions in the temperature range 20–150 °C and the pressure range 0.1–35 MPa. *J Phys Chem Ref Data.* 1981; 10(1):71–88.
30. Wang P, Anderko A, Springer RD, Young RD. Modeling Phase Equilibria and Speciation in Mixed-Solvent Electrolyte Systems: II. Liquid-Liquid Equilibria and Properties of Associating Electrolyte Solutions. *J Molec Liquids.* 2006; 125(1):37–44.
31. Wang P, Anderko A, Young RD. A Speciation-Based Model for Mixed-Solvent Electrolyte Systems. *Fluid Phase Equil.* 2002; 203(1–2):141–176.
32. Sato C, Schnoor JL, McDonald DB, Huey J. Test medium for the growth of *Nitrosomonas europaea*. *Appl Environ Microbiol.* 1985; 49(5):1101–1107. [PubMed: 16346783]
33. Soriano S, Walker N. The nitrifying bacteria in soils from Rothamsted classical fields and elsewhere. *J Appl Bacteriol.* 1973; 36(3):523–529.
34. Higgins CE, Baldwin WH, Soldano BA. Effects of Electrolytes and Temperature on the Solubility of Tributyl Phosphate in Water. *J Phys Chem.* 1959; 63(1):113–118.
35. Painter HA, Loveless JE. Effect of temperature and pH value on the growth-rate constants of nitrifying bacteria in the activated-sludge process. *Water Res.* 1983; 17(3):237–248.
36. APHA. Standard methods for the examination of water and wastewater (1989). American Public Health Association; Washington, DC: 1989.
37. Hesford E, McKay H. The influence of diluent on extraction of europium and thorium nitrates by tri-n-butylphosphate. *Trans Faraday Soc.* 1958; 45:537.
38. Gray JA, Smutz M. An equilibrium study of the chloride and nitrate systems of praseodymium and neodymium with tributyl phosphate and acid. *J Inorg Nucl Chem.* 1966; 28(9):2015–2024.
39. Rosický L, Hála J. Solvent extraction of yttrium (III) by TBP from acidic organic-aqueous solutions. *J Radioanal Nucl Chem.* 1983; 80(1):43–48.
40. Gray PR, GTS. Extraction behavior of trivalent lanthanide and actinide elements into tributyl phosphate from hydrochloric and nitric acids. US Atomic Energy Commission Document. 1952; UCRL-2069:29.
41. Engel MS, Alexander M. Growth and autotrophic metabolism of *Nitrosomonas europaea*. *J Bacteriol.* 1958; 76(2):217. [PubMed: 13563419]
42. Berne C, Allainmat B, Garcia D. Tributyl phosphate degradation by *Rhodospseudomonas palustris* and other photosynthetic bacteria. *Biotechnol Lett.* 2005; 27(8):561–566. [PubMed: 15973490]
43. Ahire KC, Kapadnis BP, Kulkarni GJ, Shouche YS, Deopurkar RL. Biodegradation of tributyl phosphate by novel bacteria isolated from enrichment cultures. *Biodegradation.* 2012; 23(1):165–176. [PubMed: 21755325]

44. Rosenberg A, Alexander M. Microbial Cleavage of Various Organophosphorus Insecticides. *Appl Environ Microbiol.* 1979; 37(5):886–891. [PubMed: 225990]
45. Thomas RAP, Morby AP, Macaskie LE. The biodegradation of tributyl phosphate by naturally occurring microbial isolates. *FEMS Microbiol Lett.* 1997; 155(2):155–159. [PubMed: 9351197]
46. Thomas RAP, Macaskie LE. The effect of growth conditions on the biodegradation of tributyl phosphate and potential for the remediation of acid mine drainage waters by a naturally-occurring mixed microbial culture. *Appl Microbiol Biotechnol.* 1998; 49(2):202–209. [PubMed: 9534259]
47. Bringmann G, Kühn R. Comparison of the toxicity thresholds of water pollutants to bacteria, algae, and protozoa in the cell multiplication inhibition test. *Water Res.* 1980; 14(3):231–241.
48. Kulkarni S, Markad V, Melo J, D'souza S, Kodam K. Biodegradation of tributyl phosphate using *Klebsiella pneumoniae* sp. S3. *Appl Microbiol Biotechnol.* 2014; 98(2):919–929. [PubMed: 23644771]
49. Andrès Y, Texier AC, Le Cloirec P. Rare earth elements removal by microbial biosorption: A review. *Environ Technol.* 2003; 24(11):1367–1375. [PubMed: 14733390]
50. Takahashi Y, Chatellier X, Hattori KH, Kato K, Fortin D. Adsorption of rare earth elements onto bacterial cell walls and its implication for REE sorption onto natural microbial mats. *Chem Geol.* 2005; 219(1–4):53–67.
51. Tsuruta T. Accumulation of rare earth elements in various microorganisms. *J Rare Earths.* 2007; 25(5):526–532.
52. Yoshida T, Ozaki T, Ohnuki T, Francis AJ. Adsorption of rare earth elements by gamma-Al<sub>2</sub>O<sub>3</sub> and *Pseudomonas fluorescens* cells in the presence of desferrioxamine B: implication of siderophores for the Ce anomaly. *Chem Geol.* 2004; 212(3–4):239–246.
53. Hu Z, Chandran K, Grasso D, Smets BF. Impact of Metal Sorption and Internalization on Nitrification Inhibition. *Environ Sci Technol.* 2003; 37(4):728–734. [PubMed: 12636271]
54. Nel A, Xia T, Mädler L, Li N. Toxic Potential of Materials at the Nanolevel. *Science.* 2006; 311(5761):622–627. [PubMed: 16456071]
55. Yuan L, Zhi W, Liu Y, Karyala S, Vikesland PJ, Chen X, Zhang H. Lead Toxicity to the Performance, Viability, And Community Composition of Activated Sludge Microorganisms. *Environ Sci Technol.* 2014; 49(2):824–830.
56. Akselrud N, Ermolenko V. Hydroxides and basic chlorides of europium, terbium and holmium. *Russ J Inorg Chem.* 1961; 6:397–399.
57. Bernkopf, MF. PhD Dissertation. Technische Universität München; 1984.
58. Smith, R., Martell, A. 4Plenum. Vol. 197. New York: Critical Stability Constants; p. 75
59. Spivakovskii V, Moisa L. Composition, activity products, and free energies of formation of scandium, yttrium, lanthanum, and lanthanide hydroxide chlorides and hydroxides. *Russ J Inorg Chem.* 1977; 22(5):643–645.
60. Davis W Jr, Mrochek J, Hardy C. The system: Tri-n-butyl phosphate (TBP)-nitric acid-water—I activities of TBP in equilibrium with aqueous nitric acid and partial molar volumes of the three components in the TBP phase. *J Inorg Nucl Chem.* 1966; 28(9):2001–2014.
61. Kertes A. Solute-solvent interaction in the system hydrochloric acid-water-tri-n-butyl phosphate. *J Inorg Nucl Chem.* 1960; 14(1):104–113.
62. Kertes A, Kertes V. Solvent extraction of mineral acids. IV. Solute-solvent interaction in the system perchloric acid-water-tri-N-butyl phosphate. *J Appl Chem.* 1960; 10(7):287–292.
63. Scargill D, Alcock K, Fletcher J, Hesford E, McKay H. Tri-n-butyl phosphate as an extracting solvent for inorganic nitrates—II Yttrium and the lower lanthanide nitrates. *J Inorg Nucl Chem.* 1957; 4(5):304–314.
64. Siekierski S. Extraction from solutions of perchloric acid by tributylphosphate—I: Partition coefficients for zirconium, thorium, cerium, promethium and yttrium. *J Inorg Nucl Chem.* 1959; 12(1):129–135.

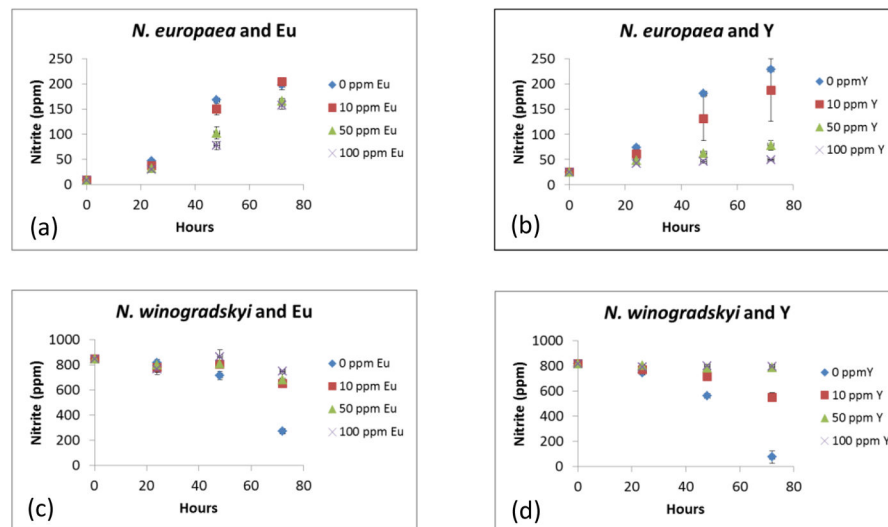


**Figure 1.** Nitrification activity for *Nitrosomonas europaea* and *Nitrobacter winogradskyi* in the presence of europium and yttrium. (a) Nitrite production by *N. europaea* in presence of Eu. (b) Nitrite production by *N. europaea* in presence of Y. (c) Nitrite consumption by *N. winogradskyi* in presence of Eu. (d) Nitrite consumption by *N. winogradskyi* in presence of Y. Error bars represent one standard deviation.

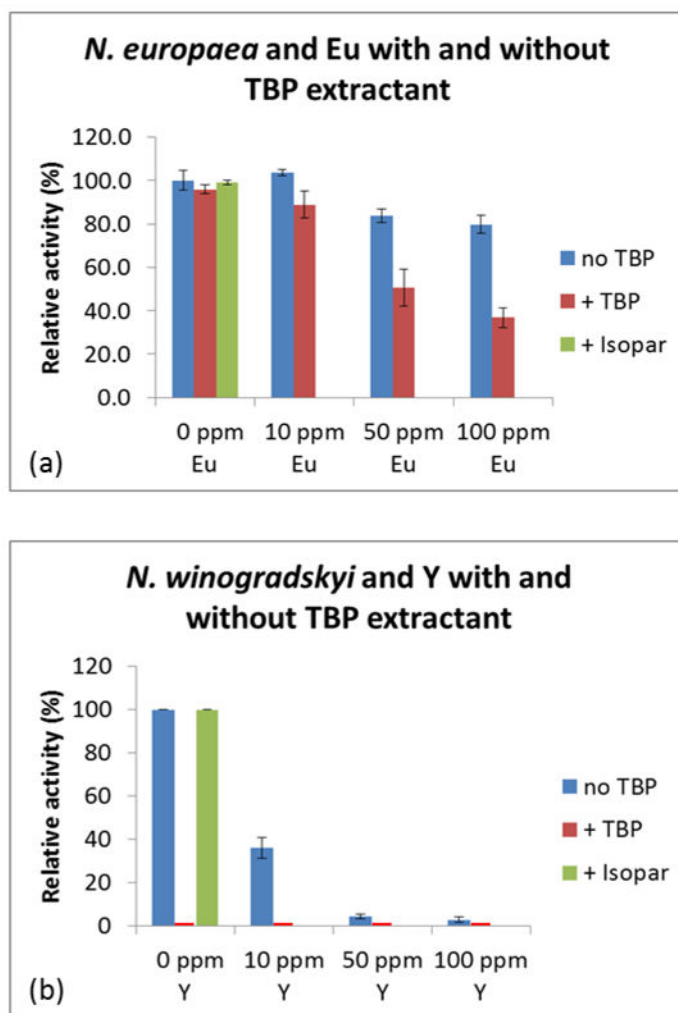


**Figure 2.** Effect of organic extractants on nitrification activity by *Nitrosomonas europaea* and *Nitrobacter winogradskyi*. (a) Relative activity compared to no Eu, no TBP control for *N. europaea*. (b) Relative activity compared to no Y, no TBP control for *N. winogradskyi*; red bars on X-axis denote absence of detectable activity in presence of TBP, regardless of level of Y addition. Note: because neither bacterium appeared to be affected by the solvent Isopar™ L, it was not tested in combination with the REE. Error bars represent one standard deviation.



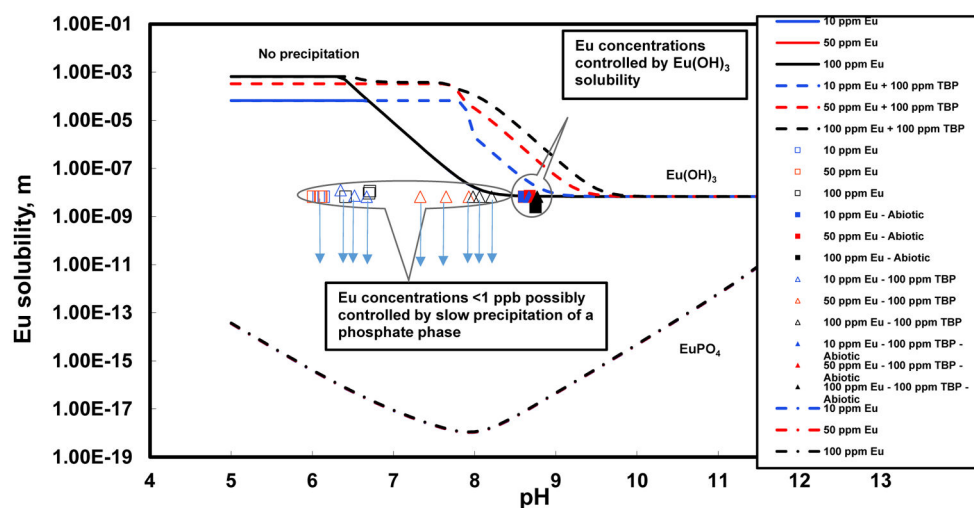


**Figure 3.** Predicted solubility of europium in the Sato <sup>32</sup> medium in the presence or absence of TBP compared to the measured concentrations as a function of pH. Symbols and curves represent experimental and predicted solubility values, respectively. Downward arrows on the symbols indicate that the values plotted are actually the detection limits; actual values for the samples were at or below these levels. The solid curves show the solubility when only  $\text{Eu}(\text{OH})_3$  precipitates. The dash-dotted curves (which all coincide) represent the solubility when both  $\text{Eu}(\text{OH})_3$  and crystalline  $\text{EuPO}_4$  can precipitate.

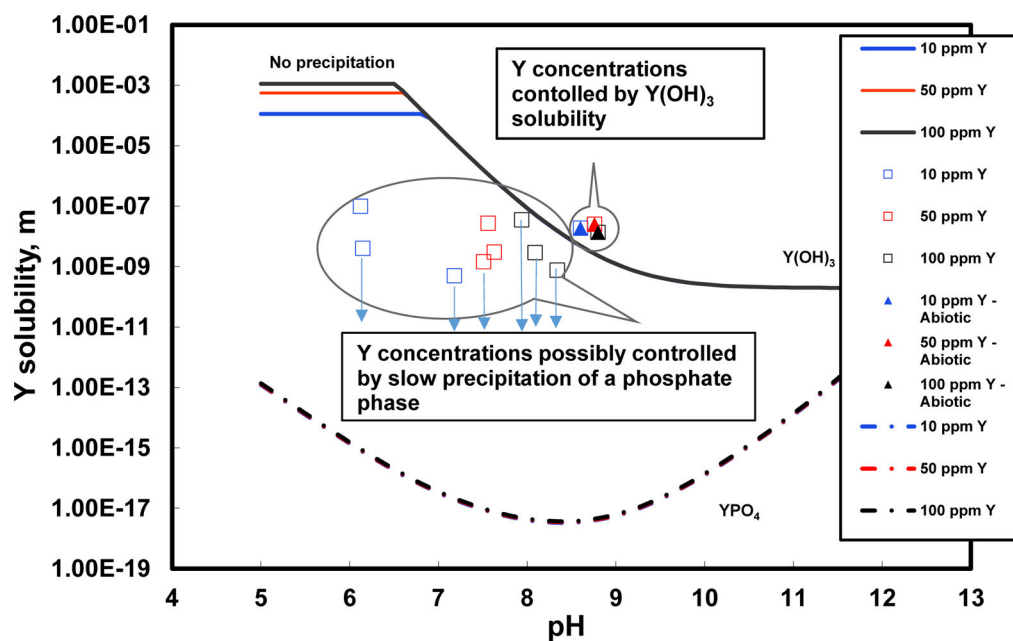


**Figure 4.** Predicted solubility of yttrium in the Sato <sup>32</sup> medium compared to the measured data as a function of pH. Symbols and curves represent experimental and predicted solubility values, respectively. Downward arrows on the symbols indicate that the values plotted are actually the detection limits; actual values for the samples were at or below these levels. The dash-dotted curves (which all coincide) represent the solubility when both  $Y(OH)_3$  and crystalline  $YPO_4$  can precipitate.

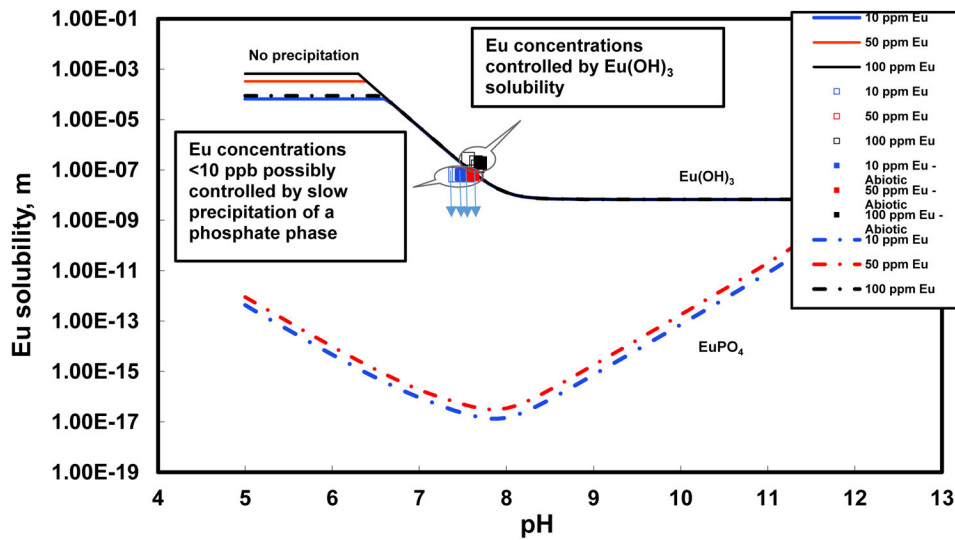


**Figure 5.** Comparison of the predicted solubility of europium in the SW<sup>33</sup> medium with the measured concentrations as a function of pH. Symbols and curves represent experimental and predicted solubility values, respectively. Downward arrows on the symbols indicate that the values plotted are actually the detection limits; actual values for the samples were at or below these levels. The solid curves show the solubility when only Eu(OH)<sub>3</sub> precipitates. The dash-dotted curves represent the solubility when both Eu(OH)<sub>3</sub> and crystalline EuPO<sub>4</sub> can precipitate (note that at 100 ppm Eu the solubility is controlled by Eu(OH)<sub>3</sub> because Eu(OH)<sub>3</sub> precipitation follows a practically complete precipitation of phosphates in the form of EuPO<sub>4</sub>).

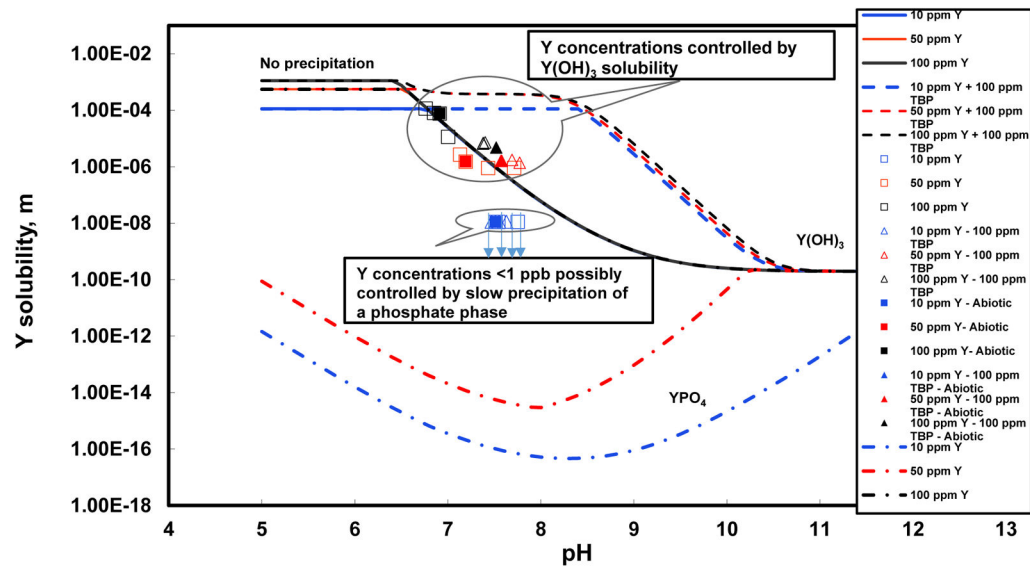


**Figure 6.** Predicted solubility of yttrium in the SW<sup>33</sup> medium in the presence or absence of TBP compared to the measured data as a function of pH. Symbols and curves represent experimental and predicted solubility values, respectively. Downward arrows on the symbols indicate that the values plotted are actually the detection limits; actual values for the samples were at or below these levels. The dash-dotted curves represent the solubility when both Y(OH)<sub>3</sub> and crystalline YPO<sub>4</sub> can precipitate (note that at 100 ppm Y the solubility is controlled by Y(OH)<sub>3</sub> because Y(OH)<sub>3</sub> precipitation follows a practically complete precipitation of phosphates in the form of YPO<sub>4</sub>).

Table 1

Sources of the experimental data used to determine the thermodynamic model parameters.

System	Data type	Temperature, °C	Pressure, atm	REE distribution coefficient range	Reference
Eu(OH) <sub>3</sub> -H <sub>2</sub> O	aqueous solubility & K <sub>sp</sub> <sup>*</sup>	25	1	-	56-58
Eu(OH) <sub>3</sub> -H <sub>2</sub> O-NaClO <sub>4</sub>	K <sub>sp</sub> & K <sub>sp</sub> <sup>*</sup>	25	1	-	57
Eu(OH) <sub>3</sub> -H <sub>2</sub> O-NaCl-NaOH	K <sub>sp</sub>	25	1	-	56, 58
Y(OH) <sub>3</sub> -H <sub>2</sub> O-NaCl	K <sub>sp</sub> <sup>**</sup>	25	1	-	59
TBP-HNO <sub>3</sub> -H <sub>2</sub> O	LLE	25	1	-	60
TBP-HCl-H <sub>2</sub> O	LLE	20	1	-	61
TBP-HClO <sub>4</sub> -H <sub>2</sub> O	LLE	27	1	-	62
TBP-HNO <sub>3</sub> -H <sub>2</sub> O-Eu	LLE-REE distribution	25	1	0.105-64	63
TBP-HNO <sub>3</sub> -H <sub>2</sub> O-Y	LLE-REE distribution	25	1	0.044-220	63
TBP-HClO <sub>4</sub> -H <sub>2</sub> O-Y	LLE-REE distribution	25	1	0.039-130	64
TBP-HCl-H <sub>2</sub> O-Y	LLE-REE distribution	25	1	0.004-19.113	Estimated <sup>§</sup>
TBP-HCl-H <sub>2</sub> O-Eu	LLE-REE distribution	25	1	0.0043-2.5976	40 + Estimated

\* Solubility product:  $K_{sp} = [Eu^{3+}][OH^-]^3$ ;  $K_{sp} = (K'_{sp})\gamma_{Eu^{3+}}(\gamma_{OH^-})^3$

\*\* Solubility product:  $K_{sp} = (K'_{sp})\gamma_{Y^{3+}}(\gamma_{OH^-})^3$

§ Data generated using the procedure explained in the supporting information